

Transverse lightwave circuits in microstructured optical fibers: resonator arrays

Maksim Skorobogatiy

*École Polytechnique de Montréal, Génie Physique, C.P. 6079, succ. Centre-Ville Montreal,
Québec H3C3A7, Canada*

maksim.skorobogatiy@polymtl.ca

<http://www.photonics.phys.polymtl.ca>

Kunimasa Saitoh and Masanori Koshiba

Division of Media and Network Technologies, Hokkaido University, Sapporo 060-0814, Japan

Abstract: Novel type of microstructured optical fiber couplers is introduced where energy transfer is enabled by transverse resonator arrays built into a fiber cross-section. Such a design allows unlimited spatial separation between interacting fiber cores which, in turn, eliminates inter-core crosstalk via proximity coupling, thus enabling scalable integration of many fiber cores. Moreover, in the limit of weak inter-resonator coupling, resonator arrays exhibit moderate polarization dependence.

© 2006 Optical Society of America

OCIS codes: (060.1810) Couplers, switches, and multiplexers; (130.3120) Resonators

References and links

1. M. Skorobogatiy, K. Saitoh, and M. Koshiba, "Transverse lightwave circuits in microstructured optical fibers: waveguides," *Opt. Express* **13**, 7506-7515 (2005), <http://www.opticsexpress.org/abstract.cfm?URI=OPEX-13-19-7506>
2. B.J. Mangan, J.C. Knight, T.A. Birks, P.St.J. Russell, and A.H. Greenaway, "Experimental study of dual-core photonic crystal fibre," *Electron. Lett.* **36**, 1358-1359 (2000).
3. B.H. Lee, J.B. Eom, J. Kim, D.S. Moon, U.-C. Paek, and G.-H. Yang, "Photonic crystal fiber coupler," *Opt. Lett.* **27**, 812-814 (2002).
4. J. Canning, M.A. van Eijkelenborg, T. Ryan, M. Kristensen, K. Lytykainen, "Complex mode coupling within air-silica structured optical fibres and applications," *Opt. Commun.* **185**, 321 (2000).
5. W.E.P. Padden, M.A. van Eijkelenborg, A. Argyros, N. A. Issa, "Coupling in a twin-core microstructured polymer optical fiber," *Appl. Phys. Lett.* **84**, 1689-1691 (2004).
6. H. Kim, J. Kim, U.-C. Paek, B.H. Lee, and K. T. Kim, "Tunable photonic crystal fiber coupler based on a side-polishing technique," *Opt. Lett.* **29**, 1194-1196 (2004).
7. J. Laegsgaard, O. Bang, and A. Bjarklev, "Photonic crystal fiber design for broadband directional coupling," *Opt. Lett.* **29**, 2473-2475 (2004).
8. K. Saitoh and M. Koshiba, "Leakage loss and group velocity dispersion in air-core photonic bandgap fibers," *Opt. Express* **11**, 3100 (2003).
9. K. Saitoh, M. Koshiba, "Full-vectorial imaginary-distance beam propagation method based on a finite element scheme: application to photonic crystal fibers," *J. Quantum Electron.* **38**, 927-933 (2002).
10. K. Saitoh, M. Koshiba, "Full-vectorial imaginary-distance beam propagation method with perfectly matched layers for anisotropic optical waveguides," *J. Lightwave Technol.* **19**, 405-413 (2001).
11. H.A. Haus, W.P. Huang, S. Kawakami, N. A. Whitaker, "Coupled-mode theory of optical waveguides," *J. Lightwave Technol.* **5**, 16 (1987).

12. M. Skorobogatiy, M. Ibanescu, S.G. Johnson, O. Weisberg, T.D. Engeness, M. Soljacic, S.A. Jacobs, and Y. Fink, "Analysis of general geometric scaling perturbations in a transmitting waveguide. The fundamental connection between polarization mode dispersion and group-velocity dispersion," J. Opt. Soc. Am. B **19**, 2867-2875 (2002).
-

1. Introduction

This work is a continuation of [1] where we have introduced the concept of transverse waveguides inside of a microstructured optical fiber (MOF) cross-section. This work addresses one of the major trends in the development of all-fiber devices - integration of multiple optical functionalities in a single fiber. The ultimate goal is being able to fabricate in a single draw a complete all fiber component provisioned on a preform level. Among others, the advantages of all-fiber devices are: simplified packaging, absence of sub-component splicing losses, environmental stability due to the absence of free space optics. Many of the interesting functionalities that fiber devices offer such as modal dispersion profile design, directional power transfer between several fiber cores [2, 3, 4, 5, 6, 7], inter-mode conversion, etc. rely critically on proximity interaction between modes localized in different spatial regions. Requirement of finite overlap of interacting modes, typically, forces multi-core systems to be designed to operate on a principle of proximity interaction, where different cores are placed in the immediate proximity of each other. Such arrangement forms an all-interacting system where all the fibers have to be considered simultaneously with a complexity of a system design increasing dramatically with the number of fiber cores. We argued that while it can be beneficial to have individual sub-components designed on a proximity principle, scalable integration of several of them in the same fiber would rather require individual spatially separated "non-interacting" sub-components and a transverse lightwave circuitry enabling connectivity between them. In [1] we have demonstrated the principles of design of the transverse lightguides that enable long range resonant energy transfer between two greatly separated cores. Such transverse waveguides were introduced by slightly changing the diameters of all the holes along the line joining the two hollow cores. We have also established that energy transfer through such a waveguide was strongly polarization dependent.

In this paper we present another type of transverse lightguides - weakly coupled resonator arrays which are considerably less polarization sensitive. We believe that such arrays is an excellent starting point for design of polarization insensitive resonant couples in the multicore MOFs.

2. Structure and definitions

In this paper we consider directional coupling between two arbitrarily far separated hollow cores in a MOF. In its traditional design two fiber cores are placed in a close proximity of each other. In such a geometry complete energy transfer from one core into the other is possible after propagation over a certain coupling length L_c , and is due to evanescent coupling of the modal fields. When two cores are spaced further apart coupling reduces dramatically resulting in an exponential increase of the coupling length making such a coupler unpractical. In what follows we demonstrate a resonant, rather than proximity, directional coupling which allows energy transfer between two fiber cores regardless of the separation between them. Moreover, suggested coupler geometry is only moderately polarization dependent. To demonstrate the robustness of our design and to investigate the importance of band gap confinement on coupler radiation losses we choose the most challenging case - design of long range coupling between two hollow core fibers guiding in the band gap of a surrounding 2D photonic crystal cladding. Structure and modal properties of individual hollow waveguides are detailed in [8]. Briefly, hollow core is formed in a silica based MOF with cladding refractive index $n = 1.45$ by re-

moving two rows of tubes and smoothing the resulting core edges. The pitch is $\Lambda = 2\mu\text{m}$, hole diameter is $d/\Lambda = 0.9$, total number of hole layers is six. Fundamental bandgap where the core guided modes are found extends between $1.29\mu\text{m} < \lambda < 1.40\mu\text{m}$. To form a coupler we place two hollow cores N periods apart from each other as in Fig. 1(a). Transverse waveguide is then introduced by slightly reducing the diameters d_w of some of the holes along the line joining the cores. In the rest of the paper we use $d_w/\Lambda = 0.7$. As hollow core size is relatively small, in order to not disturb too much guided hollow core mode we keep sizes of the $N_{wr} \geq 1$ holes closest to the cores unchanged. Periodic array of defects is then formed by reducing diameters of the appropriate holes so that the separation between them is the same and equal to $N_{rr} \geq 1$, Figs. 1(b)-(i-iii).

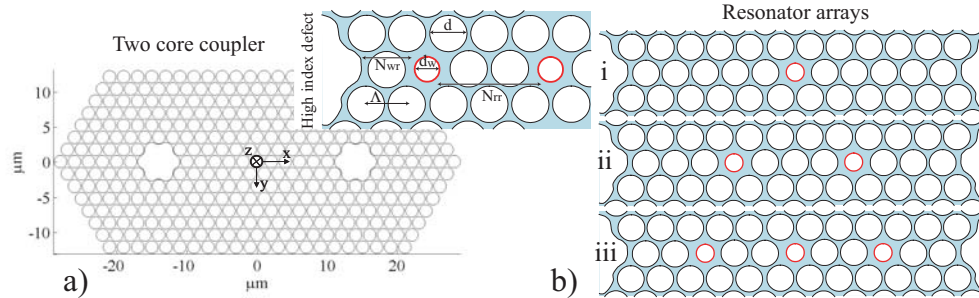


Fig. 1. Schematic of a two hollow core MOF coupler. Cores are separated by N lattice periods. Transverse waveguide is formed by a periodic array of holes of smaller diameter (resonators) separated by N_{rr} periods; N_{wr} holes closest to the cores are not modified.

In a stand alone fiber, lowest loss mode is a degenerate doublet with electric field vector having either x or y dominant component. We call such fields as x or y polarized. When second identical core is introduced, interaction between the core modes of same polarization leads to appearance of even and odd (with respect to a reflection in OY axis) supermodes with effective refractive indexes defined respectively as $n_{eff}^{x,y+}$, and $n_{eff}^{x,y-}$ closely spaced around n_{eff}^0 of a hollow core mode of a stand alone fiber. Inter-fiber coupling strength is then defined by the difference in real parts of supermode effective indexes $\Delta n_{eff}^{x,y} = |Re(n_{eff}^{x,y+} - n_{eff}^{x,y-})|$, while modal radiation losses are defined by the imaginary parts of their effective indexes. Coupling length over which power launched in one core will be completely transferred into the other one is then $L_c^{x,y} = \lambda / (2\Delta n_{eff}^{x,y})$.

Coupler radiation loss can then be estimated over a single coupling length as $P(L_c^{x,y})/P(0) = \exp(-L_c^{x,y}/L_d^{x,y})$, where power decay length is defined as $L_d^{x,y} = \lambda / (4\pi \max(Im(n_{eff}^{x,y\pm})))$. At this point a comment on the origin of a coupler loss is in order. In this paper we consider band gap guided modes that propagate above the light line of a cladding. Thus, even in the absence of material losses there will be a supermode radiation loss due to modal energy leakage into the cladding through a finite photonic band gap reflector. To counter such a radiation loss one can simply increase the number of reflector layers (layers of holes) surrounding the coupler structure. In this paper we chose to work with 6 layers which is a reasonable number for the microstructured fibers available today.

As fields of the PBG guided core modes decay exponentially fast into the photonic crystal cladding, proximity coupling between the cores will decrease exponentially fast with increase in the inter-core separation. Detailed analysis outlined above shows that for inter-fiber separation $N = 4$ coupling length is $\sim 10\text{cm}$, for $N = 7$ it is $\sim 1\text{m}$, while for $N = 11$ it is $\sim 20\text{m}$. Moreover, at a given frequency coupling lengths for different modal polarizations can differ significantly

where hollow core - resonator interaction is introduced through the coupling parameters $C_{wr}^L = \Delta H_{Lw,r}$, $C_{rw}^L = \Delta H_{r,Lw}$, $C_{wr}^R = \Delta H_{Rw,r}$, $C_{rw}^R = \Delta H_{r,Rw}$, while inter-resonator coupling is described by the parameters $C_{rr}^{RL} = \Delta H_{r_i,r_{i-1}}$, $C_{rr}^{LR} = \Delta H_{r_i,r_{i+1}}$; mode normalization is assumed to be N_i , $i = 1$. Two dominant coupling mechanisms in this system are due to the hollow core - resonator and inter-resonator interactions. Thus, without the loss of generality to make qualitative analysis simpler we further assume that six complex coupling parameters can be reduced to just two real parameters $C_{wr} = C_{wr}^L = C_{wr}^R = C_{rw}^L = C_{rw}^R$, and $C_{rr} = C_{rr}^{LR} = C_{rr}^{RL}$. Note that by choosing $C_{wr}^L = C_{wr}^R$ we have assumed that a resonator mode is even, which is typical for a fundamental mode of a stand alone waveguide. To treat odd resonator modes one has to assume $C_{wr}^L = -C_{wr}^R$. Coupling coefficients between band gap guided modes situated in different fiber cores will decrease exponentially fast with an increase in the separation between such cores. This is due to the evanescent behavior of the modal fields in the band gap cladding surrounding the cores. Note, however, that evanescent behavior of the fields is ensured by the band gap, rather than operation beyond the cladding index cut-off (as in conventional waveguides).

In the case of coupling through an array of weakly interacting resonators, supermode dispersion relations and coupling characteristics will be only moderately polarization dependent. Particularly, fundamental modes of the stand alone hollow core waveguides and resonators considered in this paper are degenerate doublets labelled as x any y polarized modes. Therefore, for a complete coupler, in the absence of interaction between coupler sub-components, the point of phase matching between the hollow waveguide and resonator modes will be the same for both polarizations. From perturbation theory it follows that in the case of a weak coupling between coupler sub-waveguides, wavelengths of the coupling resonances for both polarizations will remain close to the same phase matching frequency in the absence of coupling. Coupler polarization dependence will then arise through the polarization dependence of the normalization and coupling matrices (4) and will manifest itself in the somewhat different resonance frequencies and coupling lengths at resonance.

Finally, we would like to note that not all the modes of a resonator are degenerate doublets, some of the higher order resonator modes can be true singlets. When operating at the wavelengths corresponding to the excitation of such singlet resonator modes, coupler will exhibit strong polarization dependence. Particularly, even if the mode of operation of a hollow waveguide is a degenerate doublet supporting x and y polarizations, only one polarization of a hollow waveguide mode will be able to couple to a resonator singlet due to symmetry considerations, thus resonant coupling will only be observed for one of the polarizations. In the rest of the paper we will concentrate on the case of moderate polarization dependence of a coupler in which interaction is between the degenerate doublets of the hollow core and resonator waveguides.

In what follows, we disregard the so-called "self-slowing" terms $N_{i,j}$; $j \neq i$ due to overlap of the modes situated on the different cores. We further assume that hollow core - resonator coupling is much weaker than inter-resonator coupling $C_{wr} \ll C_{rr}$ so not to disturb considerably the fields of the hollow core modes. For the brevity of presentation, all the derivations in this paper are done for the case of an even resonator mode. With these assumptions, coupling between hollow cores mediated by a periodic resonator array can be readily understood. In Fig. 2 we present schematics of dispersion relations of the coupler supermodes modes as well as their propagation constants and expansion coefficients at a phase matching point for the case of one, two and three resonators.

3.1. Coupling via one resonator

We start with a case of two hollow cores coupled via one resonator. In Fig. 2(a) dispersion relations $\beta(\lambda)$ of the supermodes relative to a dispersion relation of a core mode of a stand alone hollow core fiber $\beta_w^0(\lambda)$ is presented. Fine black dotted line represents dispersion relation of a

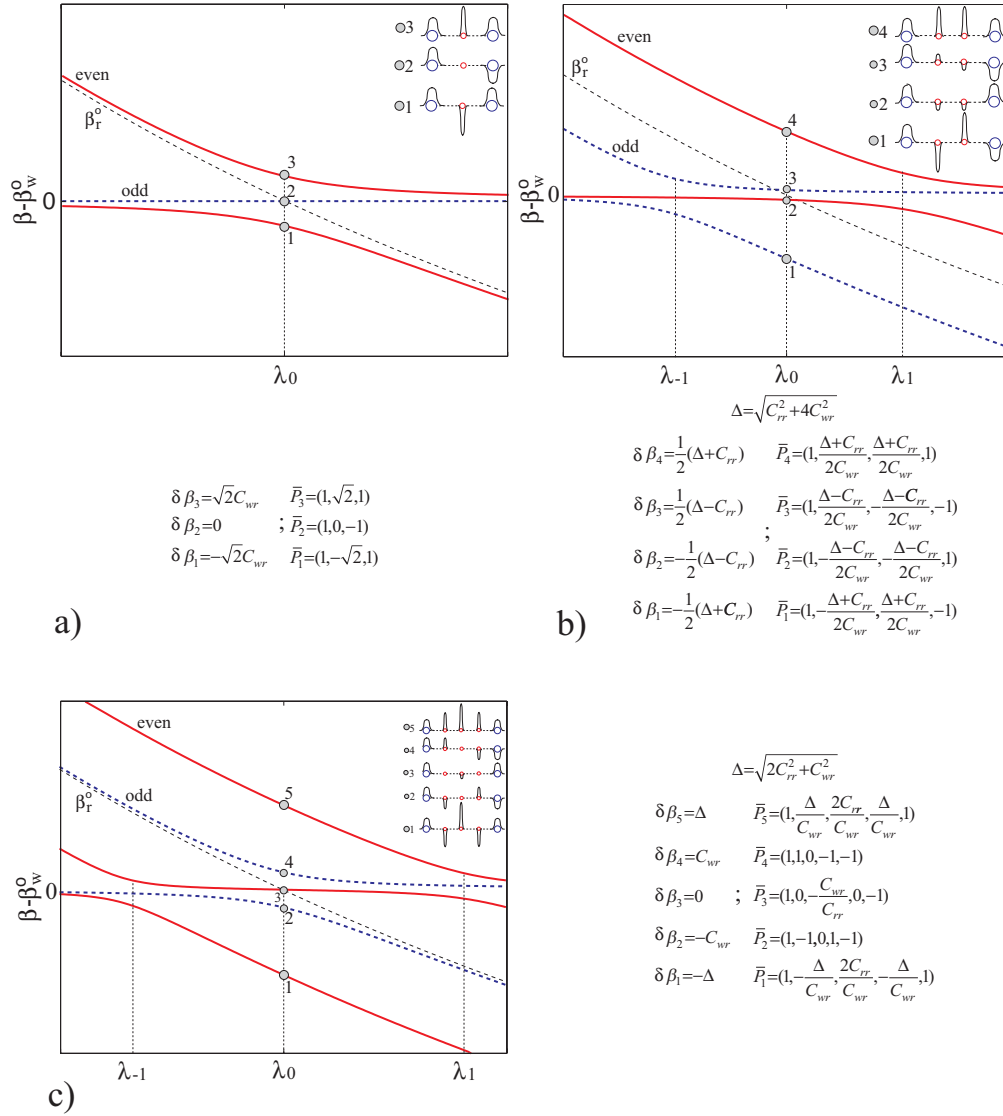


Fig. 2. Schematic of the supermode dispersion relations in weakly coupled a) 1, b) 2, c) 3 resonator arrays. Dispersion relations are plotted with respect to the one of a stand alone hollow core waveguide. Solid red curves - even supermodes, dotted blue curves - odd supermodes. Black dotted curve - dispersion relation of a fundamental mode of a stand alone resonator. Inserts - schematics of the field distributions at a phase matching point λ_0 .

guided mode of a stand alone resonator which at λ_0 is phase matched with core guided modes of the hollow waveguides. By solving eigen problem (2) near λ_0 we find that at the point of phase matching three degenerate modes split. Corresponding supermodes are formed by proper linear combinations of the three modes of the corresponding stand alone waveguides. Assuming that a resonator mode is even, then there will be one odd and two even supermodes. Field distribution in the odd supermode (dotted blue curve) presents an antisymmetric combination of the fields of the two hollow core modes with no contribution from a resonator mode. Not surprisingly, the

propagation constant of such a supermode (point 2) will be equal to the propagation constant of a mode of a stand alone hollow core fiber. The two other supermodes (red curves) will be even, exhibiting avoiding crossing in the region of phase matching. Field distributions in such supermodes show strong mixing (interaction) of the hollow core modes with the resonator modes.

In the case of two identical hollow core waveguides coupled via a single resonator complete power transfer between the hollow cores is still possible at the point of phase matching λ_0 at which distance between the points 1 and 2 is the same as the one between the points 2 and 3. At λ_0 , which we also call a resonant wavelength, we define s_1 , s_2 , and s_3 to be the fields of the supermodes with propagation constants $\beta_1 = \beta_w^0 - \sqrt{2}C_{wr}$, $\beta_2 = \beta_w^0$, and $\beta_3 = \beta_w^0 + \sqrt{2}C_{wr}$ (Fig. 2(a)). Then, linear combination $(s_1 + s_3)/2 + s_2$ corresponds to a field distribution of a core guided mode in the left hollow waveguide only. After the propagation distance $L_c = \pi/(\sqrt{2}C_{wr}) = \pi/(\beta_3 - \beta_2) = \pi/(\beta_2 - \beta_1)$, modal composition becomes $-(s_1 + s_3)/2 + s_2 \exp(j\beta_2 L_c)$, which corresponds to the field distribution of a core guided mode in the right hollow waveguide only. Note that coupling length is inversely proportional to the waveguide - resonator coupling strength.

Out of the resonance $\lambda \neq \lambda_0$ we adopt the following definition of a coupling length:

$$L_c = \lambda / (2\Delta n_{eff})$$

$$\Delta n_{eff} = \min(|\text{Re}(n_{eff}^1) - n_{eff}^2|, |\text{Re}(n_{eff}^2) - n_{eff}^3|) \quad (5)$$

BPM simulations confirm that even out of the resonance power launched into the left core reaches its maximum in the right core after propagation over such a defined coupling length (see next section). At resonance, power transfer is complete, while out of resonance only partial power transfer is observed. To characterize radiation losses of a coupler with 3 interacting modes we define power decay length L_d and power loss per one coupling length as:

$$L_d = \lambda / (4\pi \max(\text{Im}(n_{eff}^1), \text{Im}(n_{eff}^2), \text{Im}(n_{eff}^3)))$$

$$P(L_c)/P(0) = \exp(-L_c/L_d) \quad (6)$$

In Fig. 3(a) we use expressions of a supermode analysis (5,6) to predict coupling length and losses per one coupling length for a one resonator coupler showed on Fig. 1(b)-i. Recall that if no resonator were present coupling length between the two cores separated by 11 periods would be $\sim 20m$. After introduction of a resonator, coupling length is reduced by almost two decades to $7cm$ for y polarization and $12cm$ for x polarization. As expected, resonant wavelengths for the x and y polarizations are almost the same. In the lower part of Fig. 3(a) intensities of the modal electric fields are presented for a mode 1 of Fig. 2(a) showing agreement with the predictions of a coupled mode theory (2). The widths of the resonances are proportional to the hollow waveguide - resonator coupling strength C_{wr} . Total power loss over one coupling length are predicted to be 25% for y and 20% for x polarizations. Out of the resonance both coupling length and loss rapidly increase.

3.2. Coupling via two resonators

In Fig. 2(b), dispersion relation of the supermodes relative to a dispersion relation of a core mode of a stand alone hollow core fiber are shown for the case of two hollow waveguides coupled via an array of two resonators. As in the case of one resonator, at a phase matching point all the degenerate modes (two of the hollow waveguides and two of the resonators) will split by forming four properly symmetrized supermodes. Modes 1 and 4 will be split the most with a difference in their propagation constants $(\beta_4 - \beta_1) \sim C_{rr}$ being proportional to the inter-resonator coupling strength. Field distribution in these supermodes will be dominated by the

fields of the excited resonator modes. Modes 2 and 3 will be split the least with a difference in their propagation constants $(\beta_3 - \beta_2) \sim C_{wr}^2/C_{rr} \ll C_{wr}$. Field distribution in these supermodes will be dominated by the fields of the hollow waveguide core modes.

The key feature of this system is appearance of two new resonances at the wavelengths $\lambda_{\pm 1}$ corresponding to the points of avoiding crossing of the resonator supermodes 1 and 4 with the hollow core waveguide supermodes 3 and 2. In the vicinity of the resonances $\lambda_{\pm 1}$ band diagram (Fig. 2(b)) is similar to that of a single resonator coupler (Fig. 2(a)), suggesting that coupling between two hollow cores is mediated by the excitation of one of the collective resonances of a two resonator structure. As before, we define resonant wavelengths $\lambda_{\pm 1}$ as the ones at which propagation constants of the three supermodes closest to a propagation constant of a mode of a stand alone hollow core fiber are equally spaced from each other. Spacing between such resonances will be proportional to the inter-resonator coupling strength $|\lambda_{\pm 1} - \lambda_0|/\lambda_0 \sim \lambda_0 v_g C_{rr}$, where v_g is a group velocity of the resonator modes in the units of c . Same definition of coupling length as in (5) can be used to analyze power transfer between the hollow cores in the vicinity of such resonances. Complete power transfer between the hollow cores is again possible at the resonances $\lambda_{\pm 1}$, with the coupling length being inversely proportional to the hollow waveguide - resonator coupling strength $L_c \sim C_{wr}^{-1}$ and independent of the inter-resonator coupling strength.

In Fig. 3(b) we use supermode analysis (5,6) to predict coupling length and losses per one coupling length for a two resonator coupler showed on Fig. 1(b)-ii. As expected from the band diagram in Fig. 2(b), for each polarization there are two resonances with a separation between them proportional to the inter-resonator coupling strength. At such resonances, coupling length is only 2.5cm for y polarization and 5cm for x polarization. By comparison with a single resonator array we observe that coupling length at resonance for a two resonator array is further reduced due to an increase in the hollow waveguide - resonator coupling as waveguide - resonator separation N_{wr} becomes smaller (from 5 to 3). Resonant wavelengths for the x and y polarizations are somewhat different. In the lower part of Fig. 3(b) intensities of the x and y polarized modal electric fields are presented for the mode 1 of Fig. 2(b) at the resonance λ_{-1} showing an agreement with coupled mode theory predictions. Note that resonator fields in the x polarized mode (point 1_x) are extended more toward each other than corresponding fields in the y polarized modes (point 1_y), which explains why $C_{rr}^x > C_{rr}^y$; this also explains larger separation between the resonances for x polarization. The widths of the resonances are proportional to the hollow waveguide - resonator coupling strength C_{wr} which are also somewhat different for both polarizations. Total power loss over one coupling length at resonances are $\sim 6\%$ for y and 10% for x polarizations. Out of resonance, coupling length and loss of the power per coupling length rapidly increase. In between the two resonances coupling length and radiation losses remain relatively small for y polarization, while they become considerable for x polarization, making such a coupler polarization dependent.

3.3. Coupling via three resonators

In Fig. 2(c), dispersion relation of the supermodes relative to a dispersion relation of a core mode of a stand alone hollow core fiber are shown for the case of two hollow waveguides coupled via an array of three resonators. As in the case of two resonators, there are several resonant wavelengths $\lambda_{-1,0,1}$ corresponding to the points of avoiding crossing of the resonator supermodes with the hollow core waveguide supermodes. In the vicinity of the resonances band diagram is similar to that of a single resonator coupler, suggesting that coupling between two hollow cores is mediated by the excitation of one of the collective resonances of a three resonator structure. Spacing between coupler resonances will be proportional to the inter-resonator coupling strength. Complete power transfer between the hollow cores is possible at the reso-

nances, with the coupling length inversely proportional to the hollow waveguide - resonator coupling strength, and independent of the inter-resonator coupling strength.

In Fig. 3(c) we use supermode analysis (5,6) to predict coupling length and losses per one coupling length for a three resonator coupler showed on Fig. 1(c)-iii. As expected from the band diagram Fig. 2(c), for each polarization there are three resonances with a separation between them proportional to the inter-resonator coupling strength. At such resonances, coupling length is 16cm and 3cm for y polarization, and 5cm and 4cm for x polarization. Total power loss over one coupling length at resonances are 25% and 7% for y polarization, and 10% and 18% for x polarization. Out of resonance, coupling length and loss of the power per coupling length rapidly increase. In the lower part of Fig. 3(c) intensities of the x and y polarized modal electric fields are presented for the supermodes 1 and 2 of Fig. 2(c) at resonances λ_{-1} (points $1_{x,y}$ on Fig. 3(c)) and λ_0 (points $2_{x,y}$ on Fig. 3(c)) showing an agreement with coupled mode theory predictions.

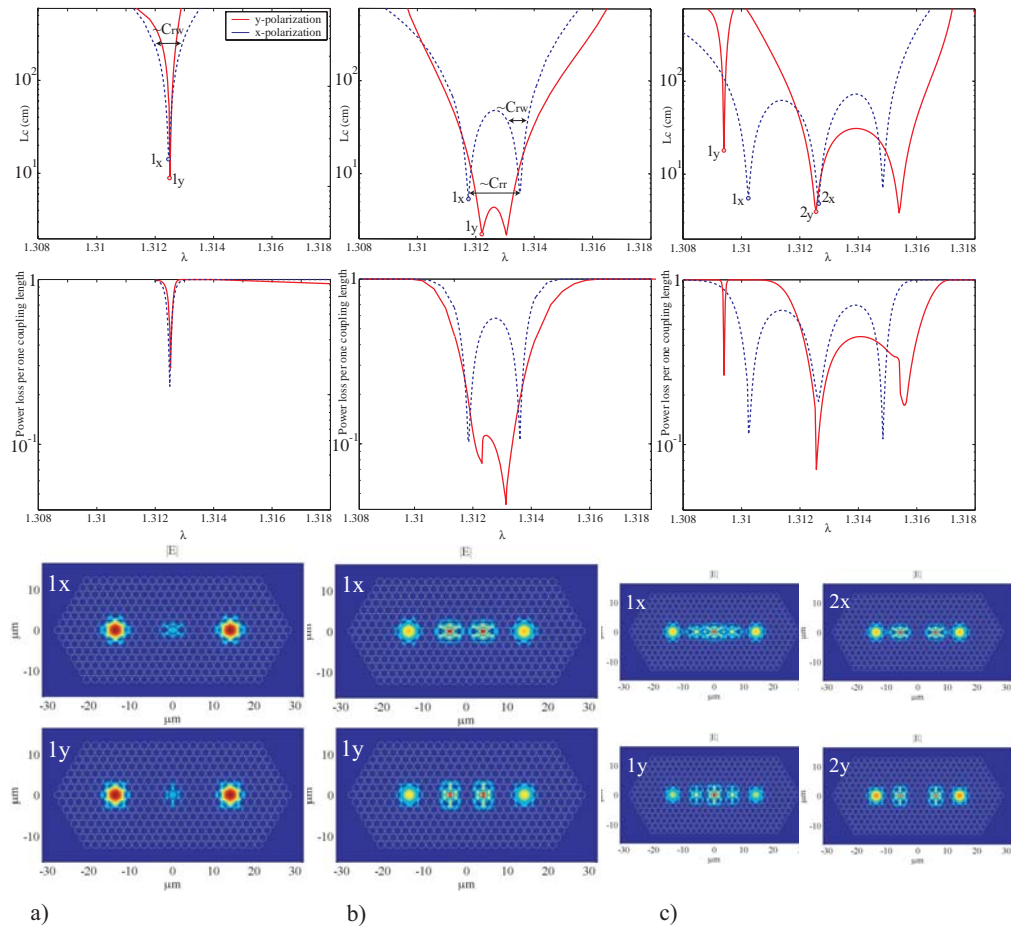


Fig. 3. Supermode analysis predictions. Coupling length, loss per one coupling length, and intensities of electric fields at resonances for the weakly coupled a) 1, b) 2, c) 3 resonator arrays. Dotted blue curves - x polarization, solid red curves - y polarization.

3.4. Coupling via more than three resonators

In a case of more than three resonators $N_r > 3$ analytical expressions for the propagation constants at a phase matching point become cumbersome. However, in the limit when $C_{wr} \ll C_{rr}/N_r$ coupling via an array of N_r resonators can still be readily understood (Fig. 4). First of all, at a phase matching point λ_0 degenerate modes will split into $N_r + 2$ supermodes. Field distribution in most of them will be dominated by various mixing of resonator modes with only a very small content of the modes of hollow waveguides; corresponding propagation constants of such modes will be close to $\beta - \beta_w^0 \simeq 2C_{rr}\sin(\pi i/(N_r + 1))$, where $i = -[N_r/2], [N_r/2]$. Field distributions in the two or three modes with the propagation constants closest to the propagation constant β_w^0 of a mode of a stand alone hollow core waveguide will exhibit strong mixing of the resonator modes with the modes of the hollow cores. In the case of even number of resonators, the split in the propagation constants of the two supermodes closest to β_w^0 will be proportional to $C_{wr}^2/C_{rr} \ll C_{wr}$. In the case of odd number of resonators (Fig. 4), the split in the propagation constants of the three supermodes closest to β_w^0 will be proportional to C_{wr} .

In spectral domain one observes appearance of N_r resonances. Spacing between such resonances will be proportional to the inter-resonator coupling strength divided by the total number of resonators, while $|\lambda_i - \lambda_0|/\lambda_0 \sim \lambda_0 v_g 2C_{rr}\sin(\pi i/(N_r + 1))$, $i = -[N_r/2], [N_r/2]$. In the vicinity of the resonances band diagram is similar to that of a single resonator coupler, suggesting that coupling between two hollow cores is mediated by the excitation of one of the collective resonances of an N_r resonator structure. Thus, at any resonance supermode analysis can be performed taking into account only three supermodes with propagation constants closest to the propagation constant of a mode of a stand alone hollow core waveguide. Such an analysis will be valid assuming that higher order modes are sufficiently far away $C_{wr} \ll C_{rr}/N_r$. Split in the propagation constants of interacting supermodes will be proportional to the hollow waveguide - resonator coupling strength C_{wr} . At such resonant wavelengths complete power transfer from one hollow core into the other is possible after propagation over a coupling length $L_c \sim C_{wr}^{-1}$ inversely proportional to the hollow waveguide - resonator coupling strength, independent of the inter-resonator coupling strength.

4. Comparison of a supermode analysis and beam propagation method

We use FEM-BMP [10] to confirm predictions of a supermode analysis for the values of coupling length and loss per coupling length defined in (5,6). To do that we revisit the case of a two resonator coupler of Fig. 1(b)-ii. In a BPM simulation we launch a mode of a stand alone hollow core fiber into the left hollow waveguide and then record total power in the hollow core of the right waveguide as a function of propagation length. Coupling length is then defined as propagation distance corresponding to the first maximum of the total power in the right hollow core. In Fig. 5(a) in solid curves we present coupling length as defined from modal analysis (5), while in dotted curves with circles coupling length is shown as calculated by BPM. Excellent agreement between the two methods is observed even outside of the resonance, suggesting that three supermode analysis is well applicable for the analysis of weakly coupled resonator arrays. Good agreement is also observed between supermode analysis prediction (6) and BPM simulations for the total power loss per one coupling length (Fig. 5(b)). In BPM the loss is given by the difference between the initial power launched into the left core and the total power left in the two cores after propagating over one coupling length.

Directly at resonance complete power transfer is expected so that after propagation over one coupling length L_c there is no power left in the left core with all the remaining power transferred into the right core. Out of resonance, only partial power transfer is expected. In Fig. 5(c) in blue dotted lines for x polarization and in red solid lines for y polarization we plot the power remaining in the left core and the power transferred into the right core after

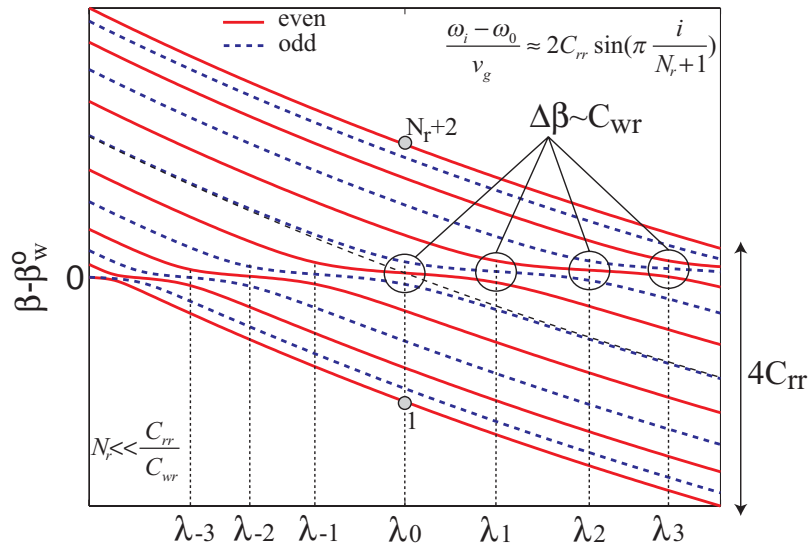


Fig. 4. Schematic of supermode dispersion relations in a weakly coupled $N_r = 11$ resonator array. Dispersion relations are plotted with respect to the one of a stand alone hollow core waveguide. Solid red curves - even supermodes, dotted blue curves - odd supermodes, black dotted curve - resonator mode in the absence of coupling. At each of the N_r coupling resonances λ_i , $i = [-5, 5]$ energy transfer from one hollow core into the other is possible via excitation of one of the collective resonance of an 11 resonator array.

propagation over one coupling length (note that at each wavelength coupling length is different Fig. 5(a)). In black lines we plot total power in the two cores remaining after propagation over one coupling length. We observe that even out of resonances, in the whole mode interaction region $1.311\mu\text{m} < \lambda < 1.314\mu\text{m}$ power transfer between the cores after one coupling length is in the range of 70 – 90%, the power remaining in the first core is in the range of 0 – 20%, while the total power loss is almost constant and equal 10%.

Necessary condition for polarization insensitive operation of a coupler is the equality of the coupling lengths for the two polarizations. In Fig. 5 thin vertical dotted lines signify two wavelengths (which we further call wavelengths of polarization insensitive operation) at which this condition is satisfied. Such wavelengths do not coincide with coupling resonances neither for x nor for y polarizations. Thus, an interesting question is to characterize partial power transfer from the left core into the right one close to the wavelengths of polarization independent operation. We demonstrate our analysis for $\lambda \simeq 1.3118\mu\text{m}$. In Fig. 5(d) in blue dotted lines with circles for x polarization and in red solid lines with circles for y polarization we plot the power remaining in the left core and the power transferred into the right core after propagation over a fixed propagation length $L_c = 10.5\text{cm}$ corresponding to the coupling length for the x and y polarized modes at the point of polarization independent operation. At resonance, for both polarizations, the transmitted power in the right core is 80% with only 5% remaining in the left core. Out of the resonance, power transfer efficiency diminishes. We call a bandwidth of such a coupler a wavelength region where the power transferred into the right core is larger than the power remaining in the left core. With this definition we find the coupler bandwidths of 0.25nm for x and 0.5nm for y polarizations. In principle, to increase coupler bandwidth one has to augment hollow waveguide - resonator coupling strength.

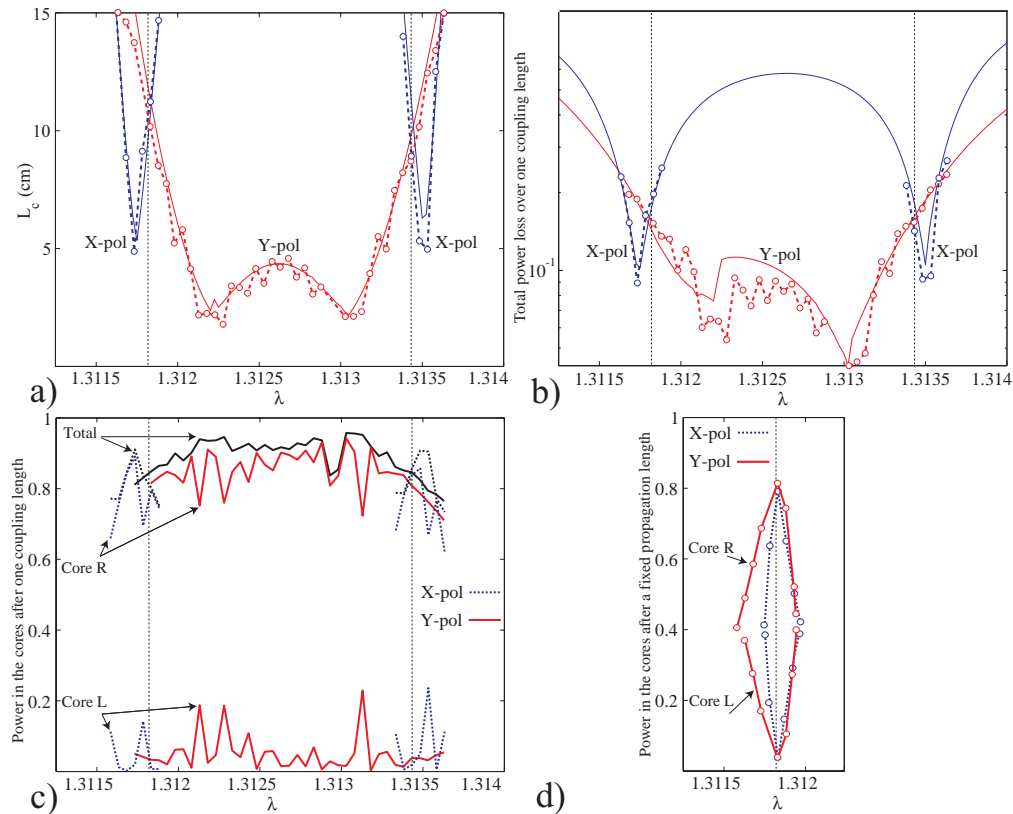


Fig. 5. Comparison between modal analysis predictions and BPM simulations for the a) coupling length, b) loss per one coupling length. Solid curves - mode analysis, dotted curves with circles - BPM. Blue curves - x polarization, red curves - y polarization; c) BPM simulations of power transfer from the left core into the right core. Blue dotted curves (x polarization) and red solid curves (y polarization) - power in the left and right cores after one coupling length; black curves - total power in both cores after one coupling length. Cyan dotted curves with circles (x polarization) and magenta solid curves with circles (x polarization) - power in the cores after propagation over a fixed distance $L_c = 10.5\text{cm}$ corresponding to a coupling length at the resonance $\lambda \simeq 1.3118\mu\text{m}$.

5. Conclusions

Novel class of microstructured optical fiber couplers is introduced that operates by resonant, rather than proximity, energy transfer via transverse resonator arrays introduced between fiber cores. Such transverse waveguides allows significant spatial separation between interacting fibers which, in turn, eliminates inter-core crosstalk via proximity coupling and allows scalable integration of multiple fiber sub-components. At resonances, controllable energy transfer of both modal polarizations between the cores is achieved over the coupling lengths of several centimeters regardless of the inter-fiber separation. Frequency separation between consecutive resonances is proportional to the inter-resonant coupling strength, while bandwidth of such a coupler at a resonance is proportional to a waveguide - resonator coupler strength. Findings based on mode analysis were confirmed by direct BPM simulations. Transmission through weakly coupled resonator array show modest polarization sensitivity making such structures a good departing point for polarization insensitive designs.